Flinders UNIVERSITY
ADELAIDE · SOUTH AUSTRALIA

Damage detection by using Scanning laser Doppler Vibrometry

By
Kaushik Prajapati

Thesis
Submitted to Flinders University
for the degree of

Master of Engineering (Mechanical)

College of Science and Engineering
06 June 2024

TABLE OF CONTENTS

ABSTRACT

This thesis investigates the application of Scanning Laser Doppler Vibrometry (SLDV) for detecting damage in an aluminium beam with a predefined notch. Structural health monitoring (SHM) is essential for maintaining the safety and integrity of mechanical systems, and noncontact methods like SLDV offer significant advantages over traditional contact-based techniques. This research aims to validate the effectiveness of SLDV in identifying structural anomalies by comparing experimental results with Finite Element Analysis (FEA) simulations.

The study involves setting up an experimental rig where an aluminium beam is vibrated using an LDS shaker system, and its out-of-plane displacement is measured using a Polytec PSV-400 SLDV system. The displacement data is processed with the Savitzky-Golay differential filter to obtain velocity curvature profiles. Parallelly, an FEA model simulates the same conditions to generate strain and deformation data, providing a basis for comparison.

Results show that SLDV effectively detects damage at lower frequencies (up to 100 Hz), where noise interference is minimal, producing sharp peaks in the velocity curvature profiles around the notch. Higher frequencies (above 100 Hz) increase Noise, making damage detection unreliable. The FEA simulations closely match the experimental data, affirming the model's accuracy and the SLDV method. However, discrepancies in noise levels between experimental and FEA results highlight the need for further refinement.

This thesis contributes to the field of SHM by demonstrating that SLDV, combined with FEA, is a reliable method for non-destructive damage detection in structural components. It emphasizes the importance of frequency selection and advanced noise reduction techniques to enhance measurement accuracy. Future research should improve noise mitigation strategies and validate SLDV against diverse structural conditions to solidify its application in real-world engineering practices.

DECLARATION

I certify that this thesis:

1. Does not incorporate without acknowledgment any material previously submitted for a degree or diploma in any university
2. and the research within will not be submitted for any other future degree or diploma without the permission of Flinders University; and
3. to the best of my knowledge and belief, does not contain any material previously published or written by another person except where due reference is made in the text.

Signature of student: Kaushik

Print name of student: Kaushikkumar Prajapati

Date: 06 June 2024

I certify that I have read this thesis. In my opinion, it is/is not (please circle) fully adequate, in scope and in quality, as a thesis for the degree of Master of Engineering (Mechanical). Furthermore, I confirm that I have provided feedback on this thesis, and the student has implemented it minimally/partially/fully (please circle).

Signature of Principal Supervisor: Stuart Wildy Digitally signed by Stuart Wildy Date: 2024.06.06 09:13:51 +09'30'

Print name of Principal Supervisor: ...Dr Stuart Wildy.....

Date: ...6/6/2024.....

ACKNOWLEDGEMENTS

I would like to express my deepest gratitude to those who have supported and guided me throughout my thesis journey.

Firstly, I extend my heartfelt thanks to my supervisor, Dr Stuart J. Wildy, for their invaluable guidance, support, and encouragement. Their expertise and insightful feedback have been instrumental in shaping this research, and their unwavering support has been a constant source of motivation.

I am immensely grateful to my family and friends for their unwavering support and encouragement. A special thanks to my wife, for her patience, love, and understanding during this journey. Your belief in me has kept me motivated and focused, and I could not have reached this point without your love and encouragement.

I also wish to acknowledge the faculty and staff of Flinders University, for their resources and expertise that have been vital to the completion of this thesis. Your assistance and support have been greatly appreciated.

Dedication

This thesis is dedicated to my father, who is no longer with us. His unwavering belief in me, his encouragement, and his sacrifices have been a constant source of inspiration. Though he is not here to see this accomplishment, his spirit and teachings continue to guide me. Thank you for instilling in me the values of hard work, perseverance, and integrity. This work is a testament to your love and support.

LIST OF FIGURES

1. INTRODUCTION

Structural health monitoring (SHM) is crucial in mechanical engineering to ensure the safety and integrity of structures. SHM is used constantly to identify damages at the initial stage to prevent catastrophic failures and minimize maintenance expenses. Detecting damage in structure in the early stage is beneficial because only a little time, money, and energy has to be invested when major issues arise.

SHM is divided into two parts: contact and noncontact techniques. Contact techniques, like strain gauges and callipers, involve touching the specimen at all tested points, which can affect surface strains and require complex setups and wiring. As a result, noncontact techniques have become preferred employment because they are simple to use and highly accurate. Such methods include the Scanning Laser Doppler Vibrometer (SLDV), which detects the frequency shift in a laser beam caused by the object's surface movement to measure the object's out-of-plane displacement and velocity (Wildy, 2012).

The main purpose of this research is to validate the effectiveness of the SLDV in detecting damage in an intentionally introduced notch on an aluminium beam. These structures are not exempt from notches that would indicate weaknesses in the structure. The study uses experimental methods and Finite Element Analysis (FEA) simulation to understand the beam's vibration response under damaged conditions. Therefore, the main objective of this paper is to show how SLDV can be used to detect structural damage and how the results of SLDV can be validated using the FEA test.

The primary goals of this research are:

- To measure the out-of-plane displacement of the aluminium beam using SLDV.
- To convert the displacement data into velocity curvature using the Savitzky-Golay equation.
- To evaluate the impact of Noise on measurement accuracy.
- The experimental data will be compared with the FEA simulation results to validate the findings.

This research uses the velocity curvature method to apply SLDV to detect damage in an aluminium beam with a predefined notch. This study explores the effect of environmental and operational Noise on SLDV measurement data and explores the Savitzky-Golay

equation method to mitigate these effects. The SLDV has significant limitations in that it is very sensitive to environmental and operational Noise.

Additionally, this study includes an FEA model to simulate the experimental scenario and obtain strain and deformation information on the beam surface. Comparing the data obtained through the Experiment with the data generated through FEA is important to validate the effectiveness of SLDV in detecting structural damage.

This thesis is significant because it applies SLDV in an experimental setup to detect damage and integrates these results with FEA simulations for validation. Driven by the interferences of Noise on the measurement data developing effective data analysis techniques, this research aims to improve the reliability of SLDV in structural health monitoring.

Knowing how Noise impacts SLDV measurements and the methods used to process it from the system is essential. This thesis needs to address more current literature by focusing on the practical application of SLDV in a noisy environment and using velocity curvature for damage detection. The findings from this research will help determine the effectiveness of SLDV and further extend the use of SLDV in the field of SHM.

This thesis demonstrates the effectiveness of scanning laser Doppler vibrometry (SLDV) in detecting structural damage. This thesis starts with an introduction highlighting the importance of structural health monitoring (SHM) and the relevance of this research. The literature review analyses the relative literature and points out the contrast in results and gaps in prior research and the strengths of SLDV over the conventional non-destructive testing techniques such as ultrasonic, eddy current and leak testing methods. The methodology describes how a notched aluminium beam was used, SLDV usage, the Savitzky-Golay filter was used, and the FEA simulation. In the results and discussion sections, experimental and FEA data were compared and summarized, and the effect of environmental Noise on measurement accuracy was investigated. In addition, velocity curvature was assessed for damage detection. The thesis closes with a comparative analysis of the findings, their relevance to SHM, and recommendations for future work, which plans to verify the proposed SLDV technique's effectiveness and improve its accuracy for structural damage identification.

2. LITERATURE REVIEWS

Background

Structural health monitoring (SJM) has evolved significantly over the years, addressing the need for reliability and evolution in NDT. Traditional methods, such as visual inspection and localized non-destructive tests, are effective. However, procedures took much time to implement and were workforce intensive and unsuitable for monitoring large structures continuously (Fan & Qiao, 2010). Vibration-based damage detection (VBDD) is the most effective methodology for SHM, and it uses changes in the dynamic properties of structures to detect the damages. VBDD is a very important application because it uses the changes in modal curvature, which is very sensitive to stiffness changes (Di Tommaso et al., 2021).

Key Authors and Methodologies

Several key authors have contributed to developing and refining curvature mode shape-based damage detection methods. In the context of curvature mode shape-based damage detection, the following scholars showed considerable contribution to the process:

WILDY (2011) highlighted the application of SLDV for identifying strain and damage with particular emphasis on displacement curvature approach. It also highlighted his work, demonstrating the full-field strain measurement using the 3D SLDV and the damage detection algorithms using displacement data.

The literature survey on vibration-based damage identification (VBDIT) techniques was presented by Fan and Qiao (2011), which categorized natural frequency, mode shape, dynamic flexibility, and modal strain energy. They also endorsed the statement that curvature mode shapes better identify damages.

These concepts were further taken to composite laminated beams by Qiao et al. (2007), who used contact (piezoelectric sensors) and noncontact SLDV. This has provided the comparison and the review of the gapped-smoothing method (GSM), generalized fractal dimension (GFD), and strain energy method (SEM) method based on the curvature mode shapes in the identification of the damages.

Lestari and Qiao (2005) chose fibre-reinforced polymer (FRP) honeycomb sandwich beams and the curvature mode shape to determine the delamination between the faceplate and the

core and the core crushing. Of course, they demonstrated that curvature mode shapes are advantageous for localized damage information.

Zhou et al. (2007), among the five VBDD methods, a comparison was made for small-scale damage detection in a bridge deck. They demonstrated that, when the shapes of the curvatures are complete, damages can be identified and localized with a limited number of measurement points. However, they admitted that considering other modes, including higher ones, would provide little improvement.

Abdel Wahab & de Rooek (1999) applied modal curvatures to estimate the damages in prestressed concrete bridges, in which they developed a Curvature Damage Factor (CDF). Their work validated the method's practicality on a real bridge, confirming its effectiveness in structural health monitoring.

In the existing research works, Hamey et al. (2004) investigated the application of curvature mode shapes for experimental damage detection in carbon/epoxy composite beams. Piezoelectric sensors and actuators were employed to capture the curvature mode shapes, and several damages identification methods were employed.

Scope and Limitations of Current Research

Curvature for identifying damage in composite structures, curvature mode shapes, has been suggested for this activity because of its high order of sensitivity to stiffness changes in the composite structure, especially for internal damages like delamination (Fan & Qiao, 2010). However, some errors arise from measurement noise, particularly at high frequencies; hence, the resolution of the sensors used in the measurement is critical. Higher-resolution sensors capture more details and, at the same may increase the system design and cost (Ručevskis & Chate, 2013). In addition, it is worth mentioning the fact that displacement curvature is used as one of the intensive approaches to the definition of vibrational intensity, and as for many surveys, the reaction on the excitation signal frequency results in several problems of comparison of the surveyed data received in different studies concerning rather high level of Noise in signals of displacement (Fan & Qiao, 2010).

Nevertheless, the potential of curvature mode shapes is known, and some concerns are regarding the future work concerning the method's standardization due to differences in the noise level of displacement signals and non-stationary characteristics of displacement curvature (Ručevskis & Chate, 2013). Based on the above analysis, it can be seen that

understanding the development needs of the measurement approaches, the decrease of the measurement noise, and the increase of curvature-based damage detection procedures are needed. (Quaranta et al., 2014).

Areas of Agreement and Disagreement

An area whereby a consensus is quickly developing among scientists is the application of curvature-based approaches for damage identification in beams. Among the identified methods, Curvature mode shape-based (CMSS) based approaches are considered sensitive to damage (Kliewer & Glisic, 2017). These methods are based on the changes in natural frequencies and modal curvatures to identify the location of damage in beams (Ta et al., 2023). Conversely, the method employing modal curvatures and the quantitative detection of the curvature slope have been used to identify the damages correctly when they exist and their location without Noise (Shi et al., 2017).

Similarly, the conflict on the right strategy for detection is also imminent. In general, some studies have pointed out that the natural frequency-based and mode shape-based methods are very effective (Fan & Qiao, 2010). Combined with the other methods using both mode shapes and frequencies, these methods have their strengths and weaknesses, and people can discuss them in the literature.

Evaluation and Critique of Literature

Using SLDV for damage identification reveals certain trends, especially in the displacement curvature approach. According to Wildy (2011) and Hou and Xia (2021), using these methods to identify structural damages is effective. However, there is a problem related to the reduction of Noisenoise and complications arising from the direct measurement of the velocity data taken by SLDV to displacement curvatures.

Another factor is noise sensitivity: the frequency-dependent Noise influences the displacement-based methods. Thus, it is not easy to compare the outcomes and reduce reliabilities. In addition, there are variations in measuring signal-to-full-scale measurement ratios, which hampers comparison of the methods. Regarding the complexity of algorithms and the use of machine learning algorithms that Hou and Xia (2021) mentioned, the limited efficiency and functionality of practical applications, especially in real-time environments, is also a downside. Most research justifies their approaches within rather real-world scenarios; they do not address how noise variations affect the reliability of the results. Also, the focus

on simple structural elements, such as beams and plates, limits the applicability to more complex structures, restricting practical utility.

Hence, a move-to-velocity curvature method is recommended because SLDV measures velocity. This approach can help eliminate Noisenoise and make analysis easier, thus increasing the level of accuracy and reliability. On these fronts, using direct velocity measurement and standardizing the metrics can fill these gaps and improve SLDV-based damage detection for real structures.

Gap Statement

The fact that researchers focus on displacement curvature while ignoring that scanning laser Doppler vibrometers directly measures velocity is a major oversight. The Noise in SLDV velocity measurement is a constant value relative to the maximum velocity measurement range. Researchers have yet to specify the signal-to-full-scale measurement ratio used in their studies. This is a significant issue as the Noisenoise within the displacement signal will vary proportionally to frequency, and many studies have compared different frequencies with constant displacement input. Therefore, there is no way to compare the effectiveness of previously published SLDV displacement curvature-based techniques. To rectify this, the study will investigate the use of velocity curvature, which will allow a direct comparison of the effect of driving frequency on the detection of damage under the same test conditions.

Scope and Limitations of Current Research

The existing literature on damage identification in structures using SLDV also involves quantifying the collected data's strain, vibration analysis, and other analytic methods. Wildy.(2011) and Hou and Xia (2021) prove the effectiveness of displacement curvature methods and machine learning to enhance accuracy.

However, there are limitations. Most of the work is concerned with displacement curvature, ignoring that SLDV obtains velocity measurements directly, which entails Noise and inefficiency. Measurement of signal to full-scale ratios makes comparing results across the studies difficult. A major disadvantage is high computational demands and testing under optimal conditions was mentioned by Fan and Qiao, (2011) and Zhou et al. (2007). Moreover, all techniques are evaluated on simple structure, which barely allows their application in complex practical situations.

3. THEORY

Velocity Curvature in Damage Detection

Displacement Curvature

Displacement curvature (κ) is one of the fundamental parameters that is used in the process of damage identification in SHM. It is calculated from the displacement field (w) of a structure and represents the second spatial derivative of this field.

$$K = \frac{\partial^2 w}{\partial x^2} \qquad \text{---------(1)}$$

Here, w is the deflection of the structure at a certain point in the length of the x. Displacement curvature depends on structure changes like cracking; therefore, it is applicable in damage identification. Nevertheless, it frequently experiences the problem of Noise, especially in the higher range, which reduces its accuracy.

Velocity

Velocity (v) is the displacement change rate with time (t). It is found by taking the first-time derivative of the displacement field:

$$v = \frac{\partial w}{\partial t} \qquad \text{---------(2)}$$

Velocity gives crucial information as to how the structure moves at that moment. SLDV measures velocity and offers a detailed view of the structure's movement without further computation to obtain displacement.

Velocity Curvature

Velocity curvature is a powerful method that includes the advantage of displacement curvature and velocity measurements. It is defined as the time derivative of displacement curvature or the second spatial derivative of the velocity field:

$$\frac{\partial \kappa}{\partial t} = \frac{\partial^2 v}{\partial x^2} \qquad \text{---------(3)}$$

This means velocity curvature helps to provide a dynamic view of structural changes, revealing how displacement curvature changes over time. Thus, this method is less sensitive to Noise and provides a more accurate measurement of velocity using data from SLDV.

Savitzky-Golay differential filter

To evaluate the out-of-plane displacement, the Savitzky-Golay differential filter is used to smooth the data and reduce Noise. The SG filter fits a low-degree polynomial to subsets of data points using linear least squares (Gorry, 1990).

The application of the 1D Savitzky-Golay differentiating filter here essentially performs a local polynomial regression (of degree n) on a distribution of $2m + 1$ points to determine the smoothed value of the r derivative of the beam deflection ($u_{z,i}$) for the length of the beam (x-direction) for each point. The one-dimensional Savitzky-Golay differentiator has the form (Wildy, 2011),

$$f_n^r(t) = \frac{1}{\Delta x^r} \sum_{i=-m}^{m} h_{t,i}^{n,r} \; u_{z,i} \tag{3.1}$$

where Δx is the distance between each data point and $h_{t,i}^{n,r}$ is the convolution weight for the data point i, with polynomial order n, and r derivative, evaluated at point t.

$$P_k^{m,r}(i) = \frac{2(2k-1)}{k(2m-k+1)}\left[iP_{k-1}^{m,0}(i) + rP_{k-1}^{m,r-1}(i)\right] - \frac{(k-1)(2m+k)}{k(2m-k+1)}P_{k-2}^{m,r}(i)$$

$$P_k^{m,r}(i) = 0 \;\; and \;\; P_{-1}^{m,r}(i) = 0$$

The Savitzky-Golay filter smooths data by fitting a polynomial of a chosen degree to a window of data points surrounding each point in the dataset. The smoothed value for each data point is then derived from this polynomial fit. The polynomial degree (n) is the degree of the polynomial used to fit the data in each window. The window size (2m + 1) is the number of data points used in each local polynomial fit. The second degree of polynomial degree and value of m is five selected in this paper. From the SLDV, displacement data $u(x,t)$ was measured at x_i, and an SG filter was applied to this data with polynomial degree 2 and a window size of 11 points. Each point fits a cubic polynomial of 11 data points and $x_i$is at the centre. This polynomial was calculated to get smooth displacement at that point (Wildy, 2011).

4. EXPERIMENTAL SETUP

An experiment was conducted to detect damage in an aluminium beam using a 1D Scanning Laser Doppler Vibrometer (SLDV). The setup included a Polytec PSV-400 SLDV system, an LDS shaker system (Appendix-A), and five notched aluminium beams. The SLDV system, which utilizes helium-neon and heterodyne interferometry, consists of a laser scanning head (PSV-400-MR), a high-resolution digital camera (A-CAZ-1000), a controller (OFV-5000), a junction box (PSV-E-401-3D), and a workstation computer (PSV-W-400-3D) (www.polytec.com, n.d.).

The laser scanning head, mounted on a tripod, directs a laser beam towards the specimen and captures the reflected beam. The camera, positioned parallel to the laser head, provides video for precise alignment. The controller processes the interferometer signal into a velocity signal, while the junction box and workstation control the laser's position, focus, and measurements, handling data acquisition and processing.

Figure 1: Experimental setup

The laser head and camera align with the measured area, as shown in Figure 2. The LDS system provides controlled sinusoidal vibrations at different frequencies to the aluminium beam, with the shaker connected to the beam's free end and the other end fixed. This setup simulates dynamic conditions to gather accurate data on the beam's vibration characteristics and strain distribution.

Specimen

In this study, an aluminium beam is utilized to replicate structural damage.

3.1 Specimen Design:

- **Material:** Aluminium, chosen for its isotropic properties and uniform response to bending strain.

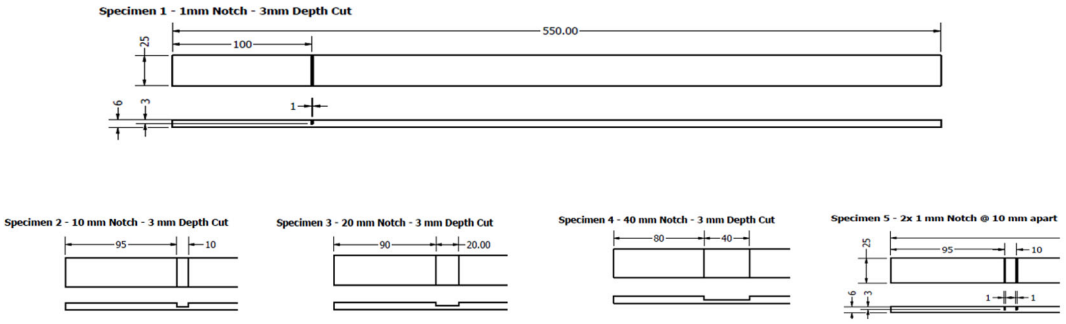

Figure 2: Specimen

- **Dimensions:** The beam is 3mm thick, 480mm Long and 25mm wide.
- **Notch:** A notch is placed in the beam to simulate damage.
    - **Specimen (a):** 1 X 1mm notch, 50 mm from fixed end
    - **Specimen (a):** 1 X 10mm notch, 45 mm from fixed end
    - **Specimen (a):** 1 X 20mm notch, 40 mm from fixed end
    - **Specimen (a):** 1 X 40mm notch, 30 mm from fixed end
    - **Specimen (a):** 2 X 1mm notch, 10mm apart, 45 mm from fixed end

The beam is clamped vertically, one end is clamped using custom-designed clamps, and the free end is connected to the LDS shaker. The beam can vibrate freely under the influence of only a shaker system. Using an LDS shaker system, a sinusoidal vibration with different frequencies was applied to the free end of the cantilever beam. This shaker provides the controlled vibrational force. The SLDV system measures the vibration response of the beam. This system scans the beam's surface and measures the out-of-plane displacement of different points along the length of the beam. 101 measurement points were created, covering a distance of 100 mm along the beam's central axis. This data is then filtered using the Savitzky-Golay filter to get velocity curvature in the in-phase quadrature.

Focusing on the beam's bottom 100 mm measurement area is very important for effective damage detection. This region experiences the highest curvature and displacement sensitivity due to the bending moment distribution in the cantilever beam. By capturing detailed curvature and displacement data in this area, the damage effects can be more accurately identified and characterized, leading to a better understanding of the beam's structural behaviour and improving the reliability of damage detection techniques.

5. EXPERIMENTAL RESULTS

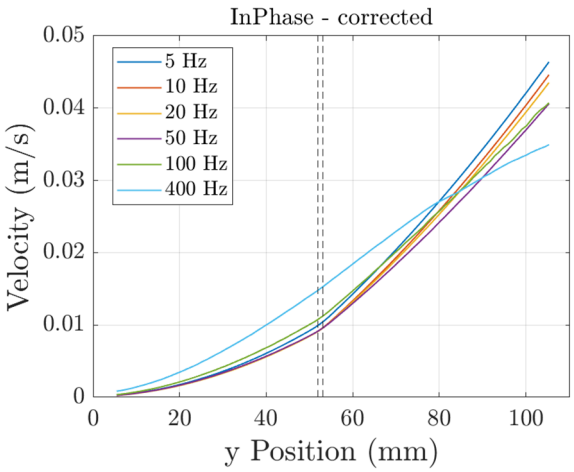

Figure 3: Max velocity at 100 mm for different frequencies

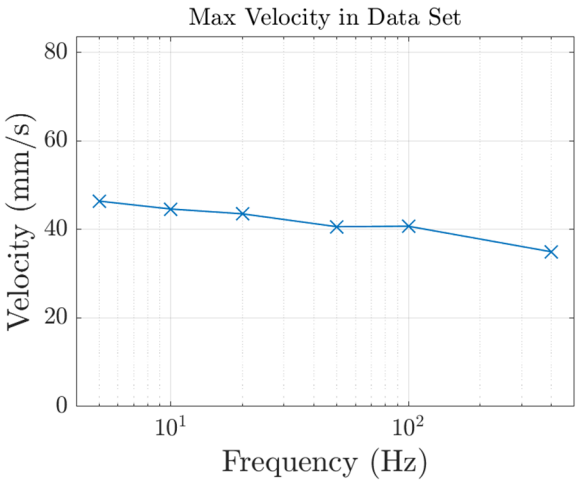

Figure 4: Velocity at different frequencies

Figure 3 shows that the velocity at the 100 mm length remained constant across different frequencies, which provides a stable reference for analyzing the beam's dynamic response. At lower frequencies like 5 Hz, 10 Hz, 20 Hz, 50 Hz, and 100 Hz, significant velocity changes along the beam's length, and slight change in curve indicate high sensitivity to structural damage, which makes these frequencies ideal for damage detection. Figure 4 shows that the maximum velocity measured at 100 mm is nearly the same for each frequency, which gives the platform for comparison of velocity curvature on constant velocity.

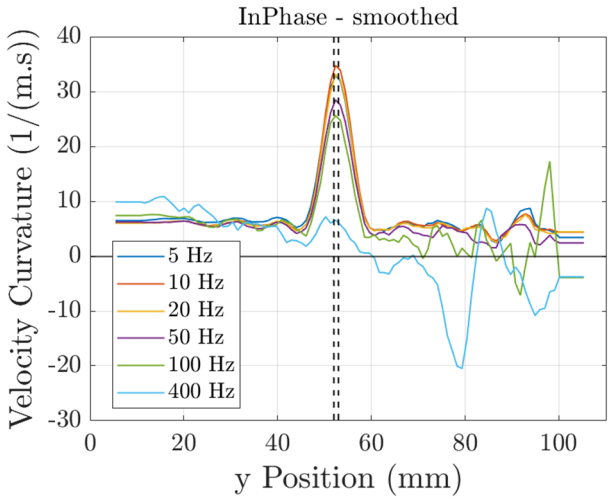

Figure 5: Velocity curvature profiles along the length of a 1 mm notched beam

Figure 5 shows the velocity curvature profiles along the length of a 1 mm notched aluminium beam for various frequencies (5 Hz, 10 Hz, 20 Hz, 50 Hz, 100 Hz, and 400 Hz). The velocity curvature data has been smoothed using the Savitzky-Golay filter with specific parameters filter size m=5, polynomial order k=2, and derivative r=2 to enhance clarity and reduce

Noise. At higher frequencies (400 Hz), the beam's velocity profiles become less damage-sensitive. The velocity changes are more gradual, and Noise has a more significant influence, reducing the effectiveness of these frequencies in detecting subtle structural changes.

The graph demonstrates that low frequencies (5 Hz, 10 Hz, 20 Hz, 50 Hz, 100 Hz) produce more pronounced and sharper peaks in the velocity curvature profiles, particularly around the 50 mm region where the 1 mm notch is located. These peaks indicate high-strain areas, suggesting the presence of damage. The effectiveness of low frequencies in damage detection is further supported by the distinct curvature changes, which are less affected by Noise.

As the frequency increases, the peaks in the velocity curvature profiles become less distinct, and the profiles exhibit more Noise. This trend indicates that higher frequencies are less effective in detecting damage due to increased noise interference, which can mask subtle structural changes.

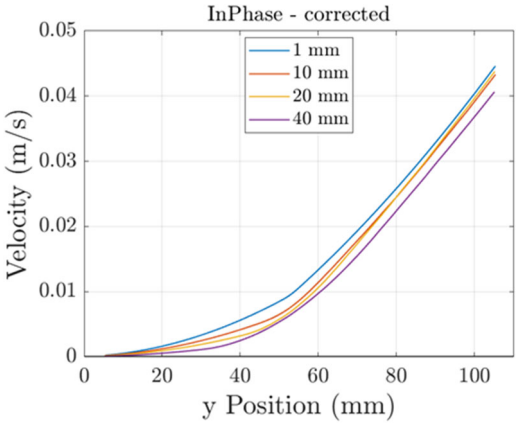

Figure 6: Velocity profiles along the length of beam at a frequency of 5 Hz for different notches

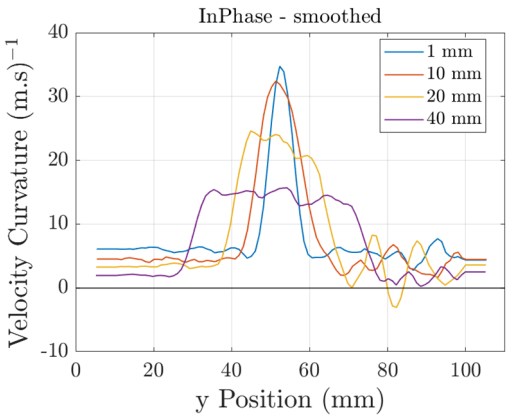

Figure 7: Velocity curvature profiles along the length of the beam at a frequency of 5 Hz for different notch sizes

Figure 6 presents the velocity profiles along the length of the aluminium beam at a frequency of 5 Hz for different notch sizes (1 mm, 10 mm, 20 mm, and 40 mm). The velocity data has been corrected for in-phase measurements to ensure accuracy.

Figure 7 shows the velocity curvature profiles (second derivative of velocity) along the length of the aluminium beam at a frequency of 5 Hz for different notch sizes (1 mm, 10 mm, 20 mm, and 40 mm), smoothed using the Savitzky-Golay filter. Appendix A provides separate graphs for each notch size at a frequency of 5 Hz.

6. FEA SIMULATION

For the Finite Element Analysis (FEA), a model of the beam was created using the ANSYS software to simulate the experimental conditions. Dimensions of the beam were 480 mm in length, 25 mm in width, and 6 mm in thickness. A notch was created as damage on the modal. The material of that beam was aluminium; its properties include a density of 2700 2700 kg/m³, Young's modulus of 70 GPa, and a Poisson's ratio of 0.33.

An experimental setup was replicated here as a cantilever configuration. At the same time, the same acceleration used in the Experiment was applied to the other end of the beam to simulate the conditions accurately.

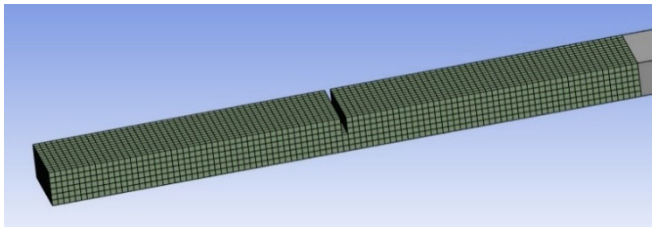

Figure 8: Mech view of the beam

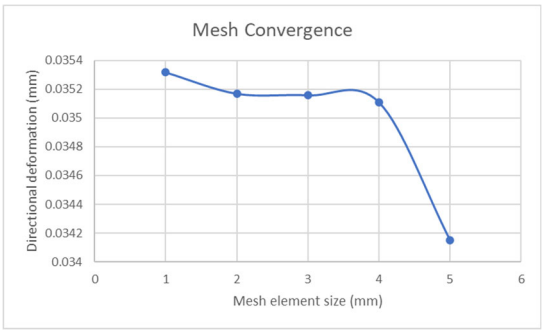

Figure 9: Mesh convergence

The hexahedral mesh was selected for the beam model because it can accurately represent the beam's geometry (Figure:8). The initial mesh size was 5 mm, and to ensure the results were not affected by the mesh size, a mesh convergence study was conducted. Element size was reduced from 5 mm to 1 mm, and harmonic analysis was conducted for each mesh size model to get displacement response. Fig 8 shows the directional deformation at different mesh sizes, and from that mesh convergence, a 1 mm mesh was selected.

A sinusoidal load with frequencies of 5 Hz, 10 Hz, 20 Hz, 50 Hz, 100 Hz, and 400 Hz was applied. The FEA included modal analysis to determine natural frequencies and mode shapes and harmonic response analysis to simulate the beam's response to the sinusoidal vibrations. The results from the FEA, displacement and strain distributions were compared with the experimental data. The comparison showed good agreement, validating the FEA model and accurately assessing the impact of the damage.

7. FEA SIMULATION RESULTS

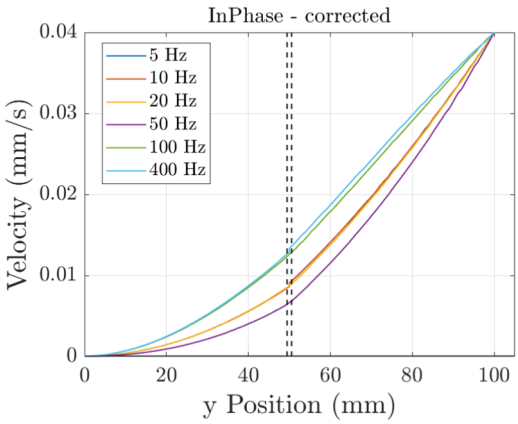

Figure 10: Max velocity at 100 mm at different frequencies.

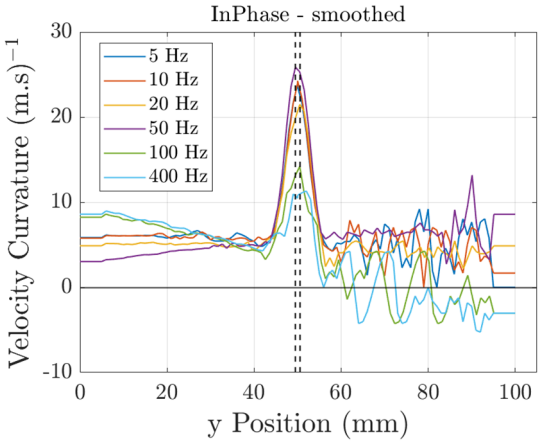

Figure 11: Velocity curvature profiles along the length of the 1mm notched beam at a different frequency

The Finite Element Analysis (FEA) simulation on an aluminium beam with a 1 mm notch was conducted at different frequencies (5 Hz, 10 Hz, 20 Hz, 50 Hz, 100 Hz, and 400 Hz) to understand the beam's behaviour and the effectiveness of these frequencies in detecting damage. The in-plane displacement data obtained from the analysis was then differentiated using the Savitzky-Golay filter to reduce Noise and differentiate the velocity to get velocity curvature. The velocity profiles at lower frequencies (5 Hz to 50 Hz) in Figure 11 showed a smooth and steady increase along the length of the beam, indicating reliable measurements with little Noise. In contrast, higher frequencies (100 Hz to 400 Hz) showed noisier profiles with more fluctuations; the reason for this is that Ansys calculates displacement, and we then convert this to velocity. This may increase the Noisenoise in the results for certain frequencies, but this Noisenoise could be reduced with increased mesh density.

The velocity curvature profiles in Figure 12 showed that low frequencies produced clear, sharp peaks around the notch region (50 mm), indicating areas of high strain and effective damage detection. However, higher frequencies resulted in significant Noise, with less clear peaks, making it harder to detect damage accurately. This analysis highlights the importance of using lower frequencies for reliable damage detection, as they provide clearer, more distinct peaks with less Noise. Individual graphs for each frequency have been attached in appendix-c

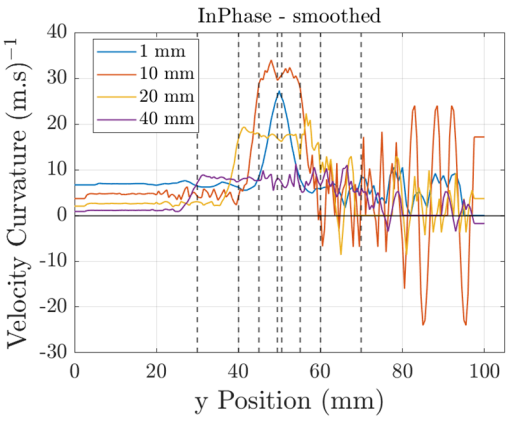

Figure 12: Velocity curvature profiles along the length of the beam at a frequency of 5 Hz for different notch sizes

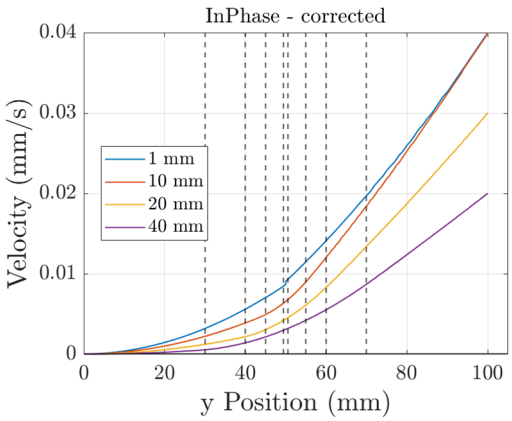

Figure 13: Velocity profiles along the length of the beam at a frequency of 5 Hz for different notch

The Finite Element Analysis (FEA) simulation at constant frequency with different notch sizes (1 mm, 10 mm, 20 mm, and 40 mm). The velocity profiles in Figure 13 showed that smaller notches (1 mm and 10 mm) resulted in higher overall velocities, indicating reliable measurements with less noise interference. Larger notches (20 mm and 40 mm) showed reduced overall velocities and more Noise, affecting the clarity of the measurements.

The velocity curvature profiles in Figure 12 show smaller notches produced sharp peaks. In comparison, larger notches resulted in broader, less pronounced peaks, indicating reduced effectiveness in identifying structural anomalies due to increased Noise and significant structural changes. So, it shows the importance of using smaller notches for reliable damage detection, as they provide clearer and more distinct peaks with less Noise. Larger notches, although detectable, introduce more Noise and structural changes, making damage detection less effective.

8. DISCUSSION

The comparative analysis of experimental and FEA results shows strong alignment in detecting damage in the notched aluminium beam, validating the FEA model. Lower frequencies are much less affected by Noisenoise and provide clear data. The Savitzky-Golay filter improved SLDV performance.

Experimental Findings:

The experimental analysis indicated that in the context of the conducted tests, at the 100 mm measurement point, the maximum velocity of the responses to various frequencies remained stable and helped to assess the dynamic behaviour of the beam. They were characterized by higher values of velocities, particularly at the lower frequencies 5 Hz, 10 Hz, 20 Hz, 50 Hz, and 100 Hz. Which shows sensitivity to changes in the wave velocity along the beam and can detect structural damage. Higher frequencies were less effective.

Velocity curvature profiles supported these results, as lower frequencies produced good peaks around the notch, indicating high-strain areas and damage. Higher frequencies had sharper peaks compared to the lower frequencies and were more noisy. At a constant frequency (5 Hz), different notches (1 mm, 10 mm, 20 mm) resulted in higher velocities with less Noise. In contrast, a big notch (40 mm) showed reduced velocities and more Noise, affecting measurement clarity. Smaller notches produced sharp peaks in velocity curvature profiles, whereas larger notches reduced the effectiveness of damage detection.

FEA Simulation Results:

The FEA simulation results aligned with the experimental findings for an aluminium beam with a 1 mm notch across various frequencies. Lower frequencies (5 Hz to 50 Hz) produced smooth velocity profiles with minimal Noise, while higher frequencies (100 Hz to 400 Hz) resulted in noisier profiles, making damage detection harder. Velocity curvature profiles at low frequencies showed clear, sharp peaks around the notch, indicating high-strain areas. For different notch sizes at 5 Hz, smaller notches (1 mm and 10 mm) produced higher velocities with less Noise, while larger notches (20 mm and 40 mm) showed reduced velocities and more Noise.

Velocity curvature profile at 5 Hz

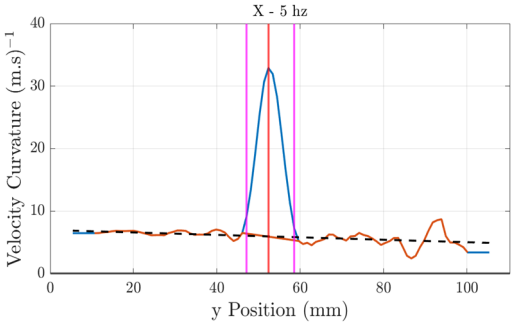

Figure 14: Velocity curvature profile of beam at 5 Hz from Experiment

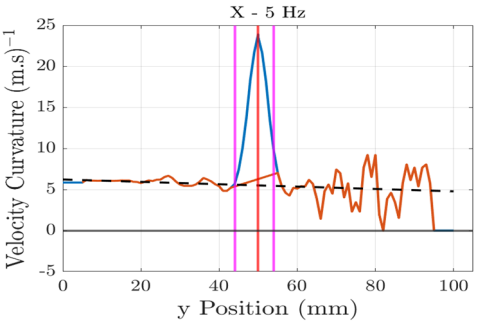

Figure 15: Velocity curvature profile of the beam at 5 Hz from FEA Simulation

The comparison between the experimental and FEA simulation results for the velocity curvature profile of the beam at 5 Hz shows a high degree of consistency. A peak detection algorithm identified the peak and peak height, with Noise calculated by comparing the signal (excluding the peak) to a fitted dashed line. Figure 14 represents the experimental results, showing a noticeable peak at 50 mm, indicating a high strain area caused by the 1 mm notch. The black dashed line represents the baseline velocity curvature, fitted to regions outside the peak, serving as a reference for the undamaged state. This clear peak demonstrates the sensitivity of 5 Hz excitation in detecting damage. Similarly, Figure 16, displaying the FEA simulation results at 5 Hz, reveals a pronounced peak in the same region (50 mm to 60 mm), indicating a high strain area due to the notch. The alignment of the peaks in both sets of results supports the accuracy and reliability of the FEA model in predicting the velocity curvature profile and detecting structural anomalies.

Noise levels in velocity curvature

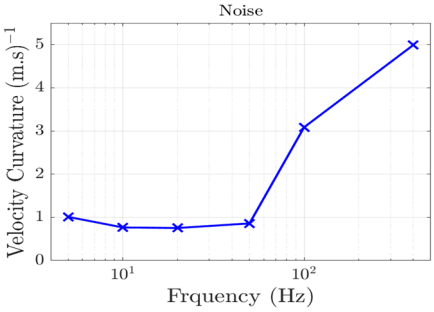

Figure 16: Noise levels in velocity curvature measured at various frequencies from experiments

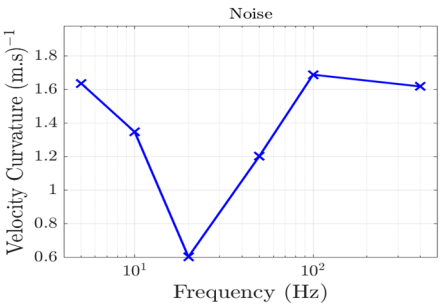

Figure 17: Noise levels in velocity curvature measured at various frequencies from FEA simulation

Figure 16 shows that experimental results at lower frequencies (up to 50 Hz) have low and stable noise levels, making them more effective for detecting structural damage with minimal interference. Noise levels sharply increase at higher frequencies, particularly above 50 Hz,

masking subtle structural changes. In contrast, Figure 17 shows that FEA simulation results exhibit a different trend, with initially high noise levels at lower frequencies, a significant dip to 0.6 (m/s)^-1 at 20 Hz, and an increase at higher frequencies. This discrepancy may arise from specific conditions and assumptions in the FEA model that only partially capture the experimental setup's complexities.

Peak heights of velocity curvature

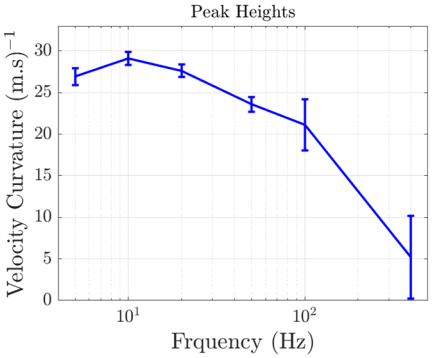

Figure 18: Peak heights of velocity curvature from from Experimental results

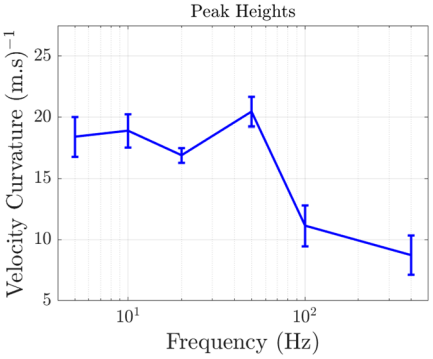

Figure 19: Peak heights of velocity curvature FEA Simulation results.

The experimental results in Figure 19 show that peak heights of velocity curvature are higher and more distinct at lower frequencies (10 Hz to 100 Hz), with values ranging from 24 to 29 (m/s)^-1, indicating significant strain and effective detection of structural issues. As frequencies exceed 100 Hz, peak heights decrease due to higher noise levels, reducing sensitivity to damage detection. Narrow error bars at lower frequencies suggest reliable, noise-affected measurements.

In contrast, the FEA simulation results in Figure 20 follow a similar trend but with generally lower peak heights, ranging from 12 to 20 (m/s)^-1 at lower frequencies. The wider error bars in the FEA results indicate more variability, suggesting the simulation might not fully capture the experimental conditions or inherent limitations in the FEA model. These differences underscore the importance of validating FEA models with experimental data. Discrepancies, such as lower peak heights and wider error bars in the FEA results, highlight areas for model refinement to improve accuracy.

The ratio of peak heights to noise levels

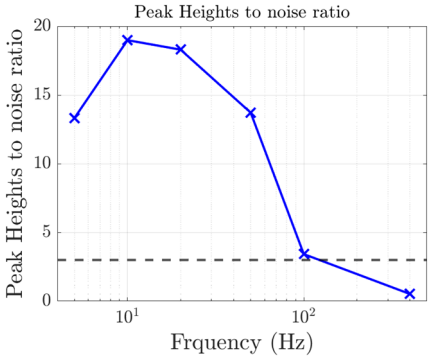

Figure 20: Ratio of peak heights to noise levels from experimental results

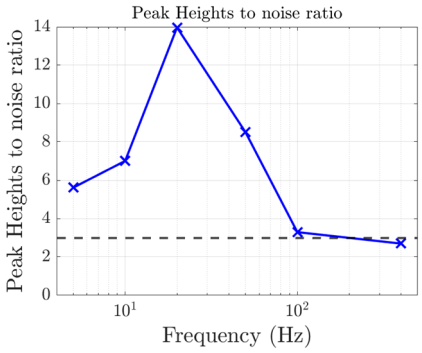

Figure 21: Ratio of peak heights to noise levels from FEA simulation results

The experimental results in Figure 21 show that the peak height-to-noise ratio is highest at lower frequencies (10 Hz to 100 Hz), with values ranging from 10 to 19. A high ratio indicates that lower frequencies are more effective for detecting damage because the signal is much stronger than the background noise. Meanwhile, the declined ratio indicates that the higher frequency is less sensitive to damage detection due to increased Noise.

The FEA simulation results in Figure 22 are similar, with high ratios at lower frequencies, and results are lower than the experimental results. At lower frequencies, the ratios range from 4 to 14, which shows that the FEA model can also predict that lower frequencies are more effective for damage detection. Both methods successfully detect the notch, which validates the use of SLDV and FEA to detect structural damage.

The difference between experimental and FEA noise levels highlights the importance of validating FEA models with experimental data. The peak at 20 Hz in the FEA results suggests a need to refine the simulation parameters to match the experimental result. These results show that lower frequencies are more effective for structural damage detection due to higher peak heights and lower noise levels. The consistency between experimental and FEA simulation results supports using FEA models to complement experimental measurements. However, there is a need for ongoing validation and refinement of FEA models to ensure their accuracy and reliability in practical applications. To improve the FEA results, fine mesh might help better capture the displacement data.

While this thesis demonstrates the effectiveness of SLDV and integration with FEA for damage detection, further research is needed. Future studies should focus on improving noise reduction techniques, especially in varying environmental conditions, to enhance the robustness of SLDV measurements.

9. CONCLUSION

This thesis shows that scanning laser Doppler vibrometry (SLDV) effectively detect damage to aluminium beams. The research confirms that SLDV and Finite Element Analysis (FEA) simulations provide a reliable, non-destructive method for structural health monitoring.

Lower frequencies are more effective for damage detection for the Experiment and FEA analysis, as they produce clear and distinct peaks in velocity curvature profiles with minimal noise interference. While useful in some contexts, higher frequencies introduced more Noise, reducing the accuracy and reliability of damage detection. The FEA simulations closely aligned with the experimental results, validating the accuracy of the SLDV method and the FEA model.

However, discrepancies in noise levels between the experimental and FEA results indicate the need for further refinement of the FEA model to capture the complexities of real-world conditions better. Applying the Savitzky-Golay filter proved beneficial in reducing Noise and improving data clarity.

Future research should focus on improving noise mitigation strategies, particularly in varying environmental conditions, to enhance the robustness of SLDV measurements further. Additionally, further validation of SLDV under diverse structural conditions is necessary to solidify its practical application in real-world engineering scenarios. By addressing these areas, SLDV can become a more reliable and widely used tool in structural health monitoring, contributing to safer and more efficient engineering practices.

10. FUTURE WORK

Future work should focus on improving noise reduction techniques and refining FEA models to better align with experimental data. Investigating a broader range of frequencies and validating results on different materials and structures will help generalise findings. Integrating SLDV with other SHM methods and developing real-time monitoring systems could enhance damage detection accuracy. Understanding the impact of environmental factors and conducting long-term studies will provide insights into damage progression. Developing user-friendly software for data analysis and quantitative damage assessment will make SLDV more accessible and practical for various applications in structural health monitoring.

BIBLIOGRAPHY

Wildy, S.J., (2012). Scanning laser Doppler vibrometry for strain measurement and damage detection (Doctoral dissertation).

Fan, W. and Qiao, P., 2011. Vibration-based damage identification methods: a review and comparative study. Structural health monitoring, 10(1), pp.83-111.

Hou, R. and Xia, Y., 2021. Review on the new development of vibration-based damage identification for civil engineering structures: 2010–2019. Journal of Sound and Vibration, 491, p.115741.

Qiao, P., Lestari, W., Shah, M.G. and Wang, J., 2007. Dynamics-based damage detection of composite laminated beams using contact and noncontact measurement systems. Journal of Composite Materials, 41(10), pp.1217-1252.

Zhou, Z., Wegner, L.D. and Sparling, B.F., 2007. Vibration-based detection of small-scale damage on a bridge deck. Journal of Structural Engineering, 133(9), pp.1257-1267.

Lestari, W. and Qiao, P., 2005. Damage detection of fibre-reinforced polymer honeycomb sandwich beams. Composite Structures, 67(3), pp.365-373.

Wahab, M.A. and De Roeck, G., 1999. Damage detection in bridges using modal curvatures: application to a real damage scenario. Journal of Sound and Vibration, 226(2), pp.217-235.

Hamey, C.S., Lestari, W., Qiao, P. and Song, G., 2004. Experimental damage identification of carbon/epoxy composite beams using curvature mode shapes. Structural Health Monitoring, 3(4), pp.333-353.

Ditommaso, R., Iacovino, C., Auletta, G., Parolai, S., & Ponzo, F. (2021). Damage detection and localization on real structures subjected to strong motion earthquakes using the curvature evolution method: the Navelli (Italy) case study. Applied Sciences, 11(14), 6496. https://doi.org/10.3390/app11146496

Ručevskis, S. and Chate, A., 2013. Damage identification in a plate-like structure using modal data. Aviation, 17(2), pp.45-51.

Quaranta, G., Carboni, B., & Lacarbonara, W. (2014). Damage detection by modal curvatures: numerical issues. Journal of Vibration and Control, 22(7), 1913-1927.

Kliewer, K. and Glisic, B. (2017). Normalized curvature ratio for damage detection in beam-like structures. Frontiers in Built Environment

Ta, D., Le, T., & Burman, M. (2023). Enhanced single damage identification in beams using natural frequency shifts and analytic modal curvatures. Journal of Science and Technology in Civil Engineering (Stce) - Huce, 17(1)

Shi, J., Spencer, B., & Chen, S. (2017). Damage detection in shear buildings using different estimated curvature. Structural Control and Health Monitoring

Hamey, C., Lestari, W., Qiao, P., & Song, G. (2004). Experimental damage identification of carbon/epoxy composite beams using curvature mode shapes. Structural Health Monitoring, 3(4), 333-353.

Qiao, P., Lestari, W., Shah, M., & Wang, J. (2007). Dynamics-based damage detection of composite laminated beams using contact and noncontact measurement systems. Journal of Composite Materials, 41(10), 1217-1252.

Gorry, P.A. (1990). General least-squares smoothing and differentiation by the convolution (Savitzky-Golay) method. *Analytical Chemistry*, 62(6), pp.570–573.

www.polytec.com. (n.d.). *Vibrometry products - PSV-500 Polytec Scanning Vibrometer - Polytec*. [online] Available at: https://www.polytec.com/int/vibrometry/products/full-field-vibrometers/psv-500-scanning-vibrometer [Accessed 19 May 2024]

APPENDICES

Appendix: A

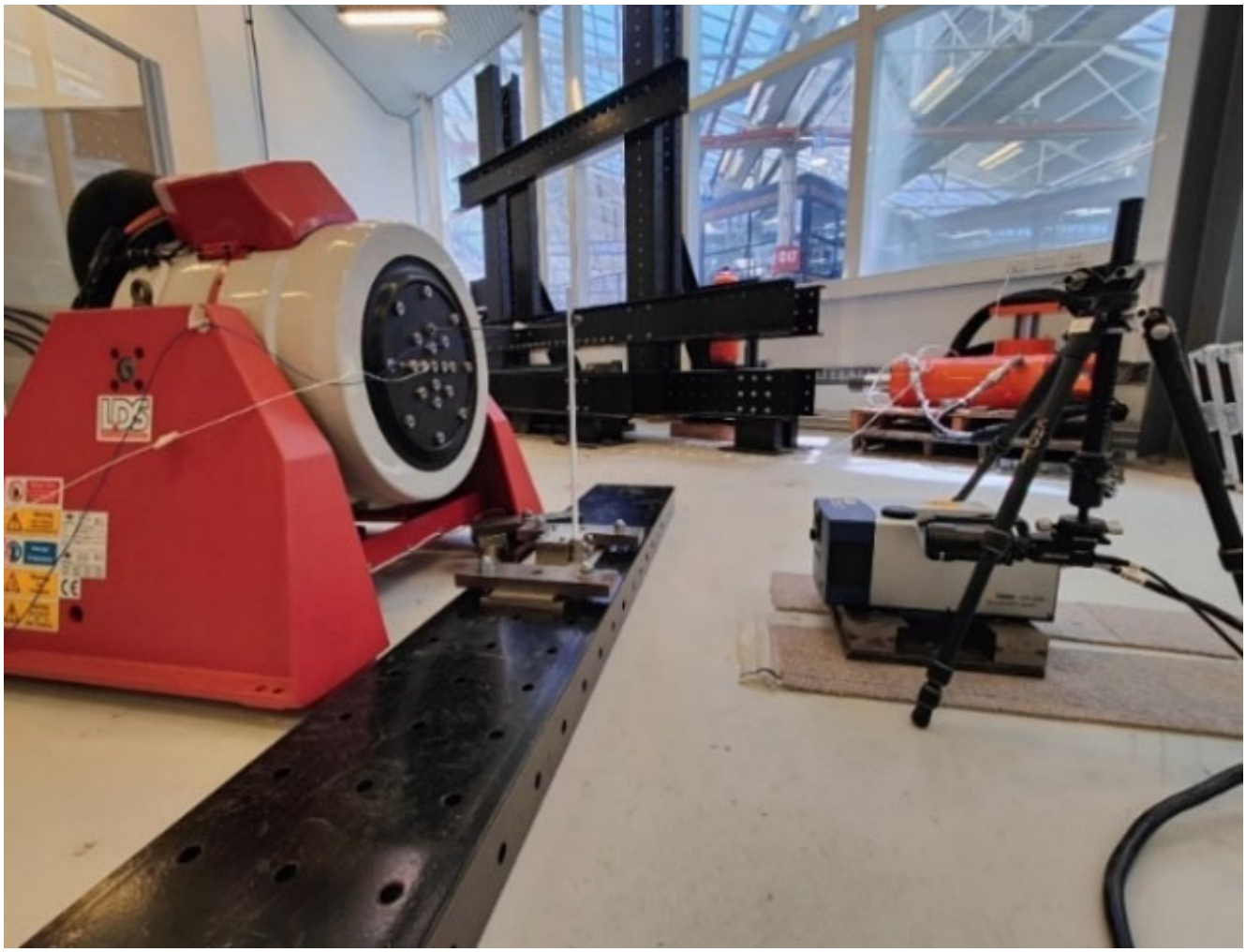

Figure 22: Experimental setup

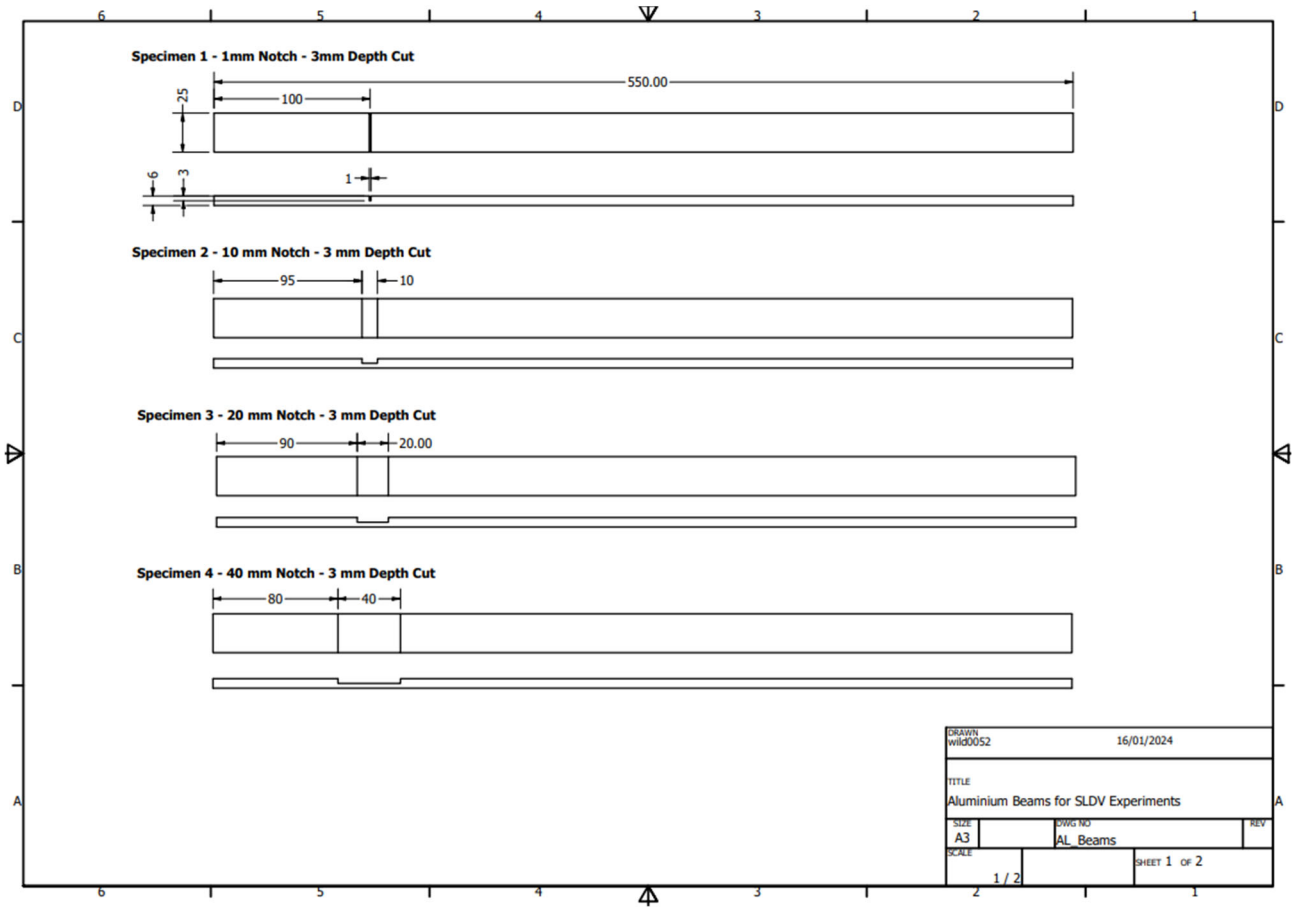

Figure 23: Specimen engineering drawing

Technical Data

Standard System Components	
Vibrometer system	■ OFV-5000 Vibrometer Controller, equipped with analog (PSV-400-B) and additional digital velocity decoder (M2-20: with analog displacement decoder) ■ PSV-I-400 Sensor Head, includes OFV-505 Vibrometer Sensor, precision scanner and color video camera with autofocus and 72X zoom, with transportation case ■ PSV-E-401 Junction Box with PSV-CL-10 main cable, 10 m
Computer	■ PSV-W-401 Data Management System ■ Industrial PC with Windows® XP or Visita 64, Gigabit Ethernet, data aquisition hardware ■ 24" Wide screen monitor, DVD writer, optical mouse and keyboard
Accessories	■ VIB-A-T02 Tripod with tip-tilt adapter ■ PSV-Z-051 Handset (optional for PSV-400-B)

Additional components depend upon PSV model and configuration

Optics			
Component	PSV-I-400 Sensor Head	PSV-A-420 Geometry Scan Unit (optional) with PSV-I-400	PSV-A-410 Close-up Unit (optional)
Dimensions [W x L x H]	190 mm x 376 mm x 163 mm (7.5 in x 14.8 in x 6.4 in)	238 mm x 376 mm x 163 mm (9.4 in x 14.8 in x 6.4 in)	124 mm x 90 mm x 75 mm (4.9 in x 3.5 in x 3.0 in)
Weight	7 kg (15.4 lbs)	7.4 kg (16.3 lbs)	0.35 kg (0.77 lbs)
Laser type	HeNe laser (633 nm)	Laser diode (620 ... 690 nm)	–
Laser safety class	Class 2 (<1 mW visible output)	Class 2 (<1 mW output)	–
Working distance	With MR lens: 0.04 m...–100 m; with LR lens: 0.35 m...–100 m		> 152 mm
Sample size	From few mm² up to several m²		
Camera	Color video camera, CCD 1/4", 752x582 pixels, with Auto Focus and 72X Zoom (4X digital, 18X optical)		
Scanner	High precision scan unit (scanning range ±20° about X,Y); angular resolution <0.002°, angular stability <0.01°/hr		
Scan speed	Up to 30 points/s (typical)		

Data Acquisition/Data Processing					
Component		OFV-5000 Vibrometer Controller	PSV-E-401 Junction Box	PSV-E-408 Junction Box (optional for H-system)	PSV-W-401 Data Management System
Dimensions [W x L x H]	mm (in)	450 x 360 x 150 (17.7 x 14.1 x 5.9)	450 x 360 x 135 (17.7 x 14.1 x 5.3)	482 x 303 x 23 (19.0 x 11.9 x 0.9)	450 x 550 x 190 (17.7 x 21.7 x 7.5)
Weight		10 kg (22.0 lbs)	9 kg (19.8 lbs)	1.5 kg (3.3 lbs)	18 kg (39.7 lbs)

General Specifications	
Power	100 VAC...240 VAC ±10 %, 50/60 Hz; overall max. 800 W
Environmental conditions	Operating temperature: +5 °C ... +40 °C (41 °F ... 104 °F); storage temperature –10 °C ... +65 °C (14 °F ... 149 °F); relative humidity: max. 80 %, non-condensing
Calibration	Every 24 months (shorter re-calibration intervals available upon request)

PSV-400 Decoder/Performance Specifications						
Model	Decoder	# of ranges	Ranges mm s⁻¹/V	Full scale (p) m/s	Decoder frequency range	Resolution[1] µm s⁻¹ /√Hz
PSV-400-B	VD-04	3	10 ... 1000	0.1 ... 10	0.5 Hz ... 250 kHz	0.1 ... 5
PSV-400-H4	VD-08	8	0.2 ... 50	0.002 ... 0.5	DC ... 25 kHz	< 0.01 ... 0.2
	VD-09	8	5 ... 1000	0.05 ... 10	DC ... 2.5 MHz	0.01 ... 4
PSV-400-H4-S	VD-03-S	3	20 ... 2000	0.2 ... 20	0.5 Hz ... 1.5 MHz	0.1 ... 5
	VD-07-S	6	2 ... 100	0.02 ... 1	DC ... 350 kHz	<0.05 ... 0.2
PSV-400-M2	VD-07	6	1 ... 50	0.01 ... 0.5	DC ... 350 kHz	<0.02 ... 0.2
PSV-400-M4	VD-09	8	5 ... 1000	0.05 ... 10	DC ... 2.5 MHz	0.01 ... 4
PSV-400-M4-S	VD-09-S VD-07-S	14	10 ... 2000	0.1 ... 20	DC ... 2.5 MHz	0.04 ... 8
PSV-400-M2-20 additionally	VD-05[2]	2	100/500	nom. 0.5/2.5	0.5 Hz ... 10 MHz	<3
	DD-300[2]	1	50 nm/V	75 nm[3]	30 kHz ... 24 MHz	<0.02 pm /√Hz[4]
Optional[5]	DD-900	16	0.05 ... 5000 µm/V	1 µm ... 100 mm[6]	DC ... 2.5 MHz	<0.015 ... 1500 nm[7]

Figure 24: Technical data of SLDV (PSV-400-MR)

V830 and V850 Shaker Specification

Shaker Model	V830-185	V830-335	V850-240	V850-440
Armature Diameter	185 mm (7.28 in)	335 mm (13.19 in)	240 mm (9.45 in)	440 mm (17.32 in)
Usable Frequency Range *	dc to 3500 Hz	dc to 3000 Hz	dc to 2600 Hz	dc to 3000 Hz
Armature Resonance (fn)	3100 Hz	2250 Hz	2400 Hz	2200 Hz
Acceleration (sine peak)†▪	1176 m/s² (120 gn)	810 m/s² (83 gn)	1225 m/s² (125 gn)	932 m/s² (95 gn)
Acceleration Random (rms)†	735 m/s² (75 gn)	588 m/s² (60 gn)	588 m/s² (60 gn)	490 m/s² (50 gn)
Effective Mass of Moving Elements				
Armature fitted with Flush Inserts	7.0 kg (15.4 lb)	12.0 kg (26.6 lb)	14.0 kg (30.9 lb)	23.8 kg (52.6 lb)
Armature fitted with Raised Inserts	7.5 kg (16.5 lb)	12.8 kg (28.3 lb)	14.3 kg (31.6 lb)	24.5 kg (54.1 lb)
Suspension Rotational Stiffness	41.8 kN m/rad (30 800 lbf ft/rad)	67.8 kN m/rad (50 000 lbf ft/rad)	57.4 kN m/rad (42 300 lbf ft/rad)	90.0 kN m/rad (66 700 lbf ft/rad)
Suspension Axial Stiffness	Nil		Nil	
Suspension Cross-axial Stiffness	5.25 kN/mm (30 000 lbf/in)		6.65 kN/mm (38 000 lbf/in)	
Internal Load Support Capability	160 kg (350 lb)		350 kg (770 lb)	
Stray Magnetic Field§	< 0.5 mT (5 gauss)		< 1.8 mT (18 gauss)	
Velocity (sine peak)†	2.0 m/s (78.7 in/s)			
Displacement (peak-peak)‡	50.8 mm (2.0 in)			
Body Suspension Resonance	Lin-E-Air Suspension: < 5 Hz — Air Isolaton Mounts: < 10 Hz			
Ambient Working Temperature	+7 to 30 °C (+45 to 86 °F)			
Body Mass	Solid Trunnions: 616 kg (1358 lb) Lin-E-Air Trunnions: 454 kg (1000 lb)		Solid Trunnions: 1288 kg (2840 lb) Lin-E-Air Trunnions: 1125 kg (2480 lb)	
Maximum Dimensions (H x W x D)	Solid Trunnions: 838 x 1005 x 772 mm (33.0 x 39.6x 30.4 in) Lin-E-Air Trunnions: 837 x 942 x 600 mm (33.0 x 37.1 x 23.6 in)		Solid Trunnions: 838 x 1246 x 1094 mm (33.0 x 49.1 x 43.1 in) Lin-E-Air Trunnions: 838 x 1165 x 849 mm (33.0 x 44.0 x 29.7 in)	

* Displacement will be limited below body suspension resonance due to body movement. Recommended min Freq base mount 8 Hz. Lin-E-Air 5Hz.
† Velocity and acceleration ratings depend on the amplifier driving the shaker.
▪ With flush inserts. 335mm/440mm armature with multi point control.
‡ Displacement can vary with payload and shaker orientation. Please contact Brüel & Kjær for advice on specific test requirements.
§ Theoretical maximum, measured 150mm (6 in) above table, full-field, at normal operation temperature.

Figure 25: LDS V830 Shaker system specification

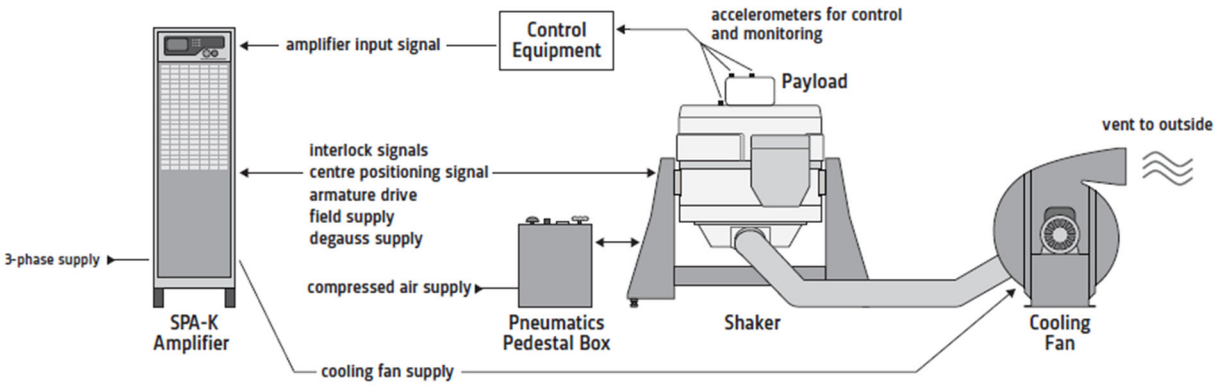

Figure 26: Typical LDS Shaker system

Appendix: B

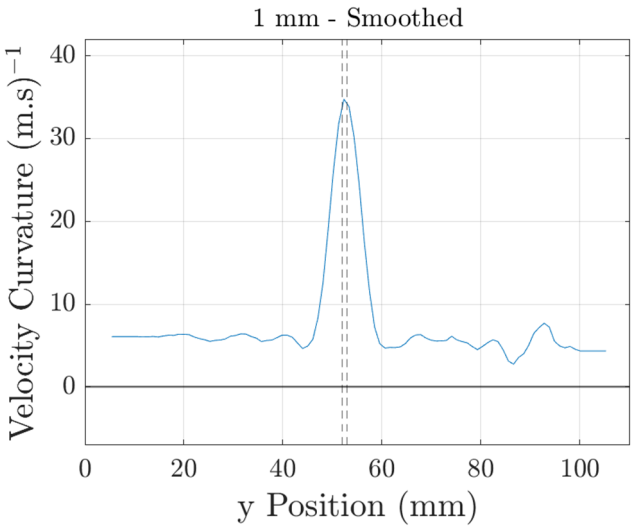

Figure 27: Velocity curvature for 1 mm notched beam at 5 Hz frequency

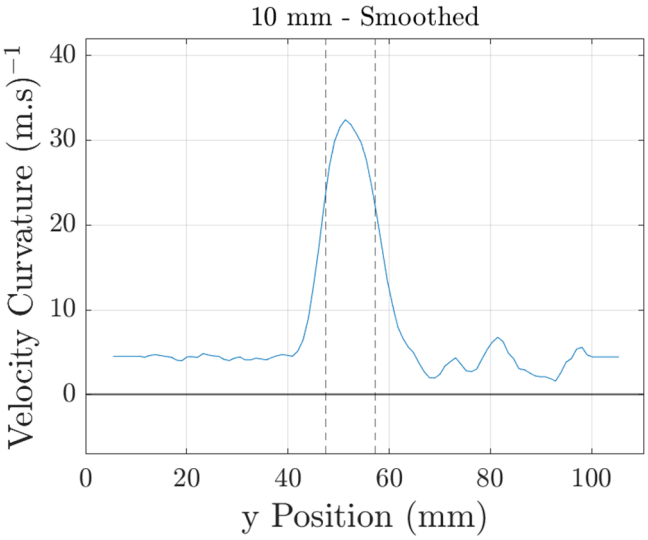

Figure 28: Velocity curvature for 10 mm notched beam at 5 Hz frequency

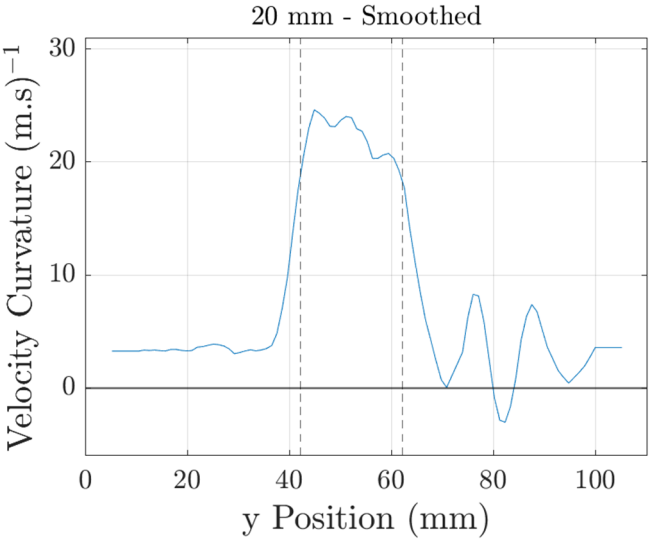

Figure 29: Velocity curvature for 20 mm notched beam at 5 Hz frequency

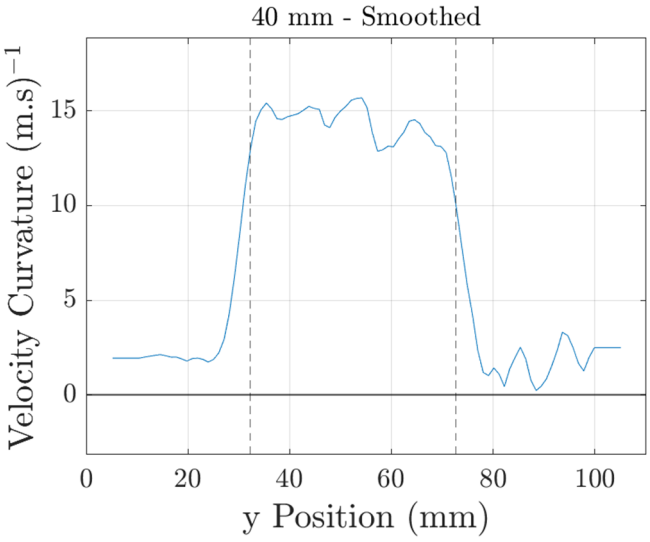

Figure 30: Velocity curvature for 40 mm notched beam at 5 Hz frequency

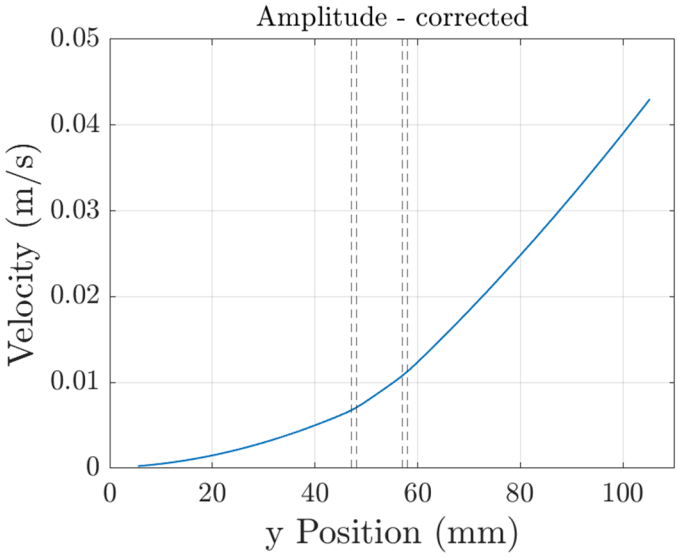

Figure 31: Velocity graph for two 1 mm Notches 10 mm apart beam at 5 Hz frequency

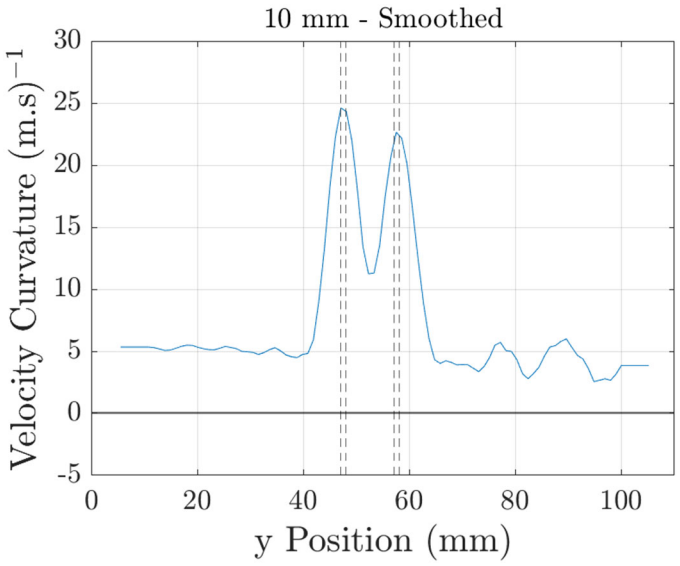

Figure 32: Velocity curvature for two 1 mm Notches 10 mm apart beam at 5 Hz frequency

Appendix: C

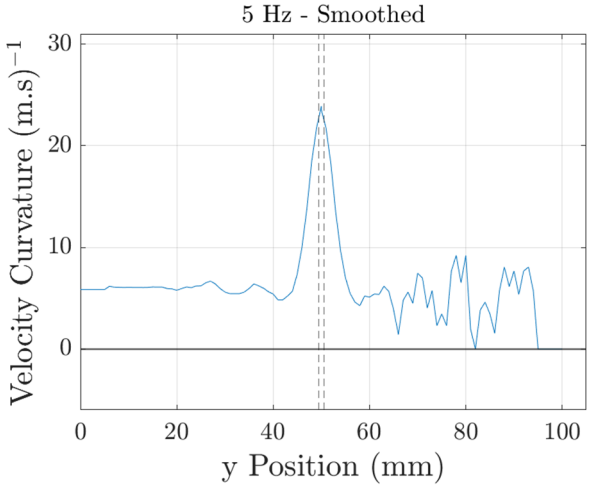

Figure 33: Velocity curvature for 1 mm notched beam at 5 Hz frequency from FEA simulation result

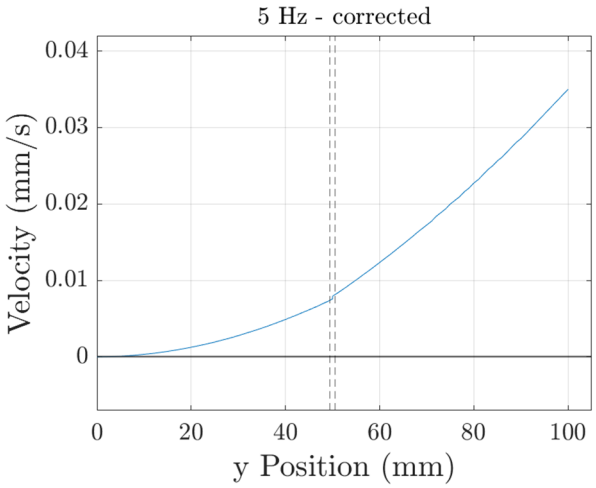

Figure 34: Velocity graph for 1 mm notched beam at 5 Hz frequency from FEA simulation result

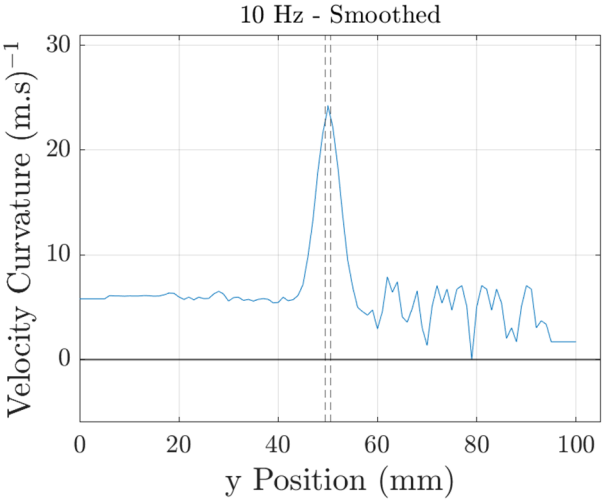

Figure 35: Velocity curvature for 1 mm notched beam at 10 Hz frequency from FEA simulation result

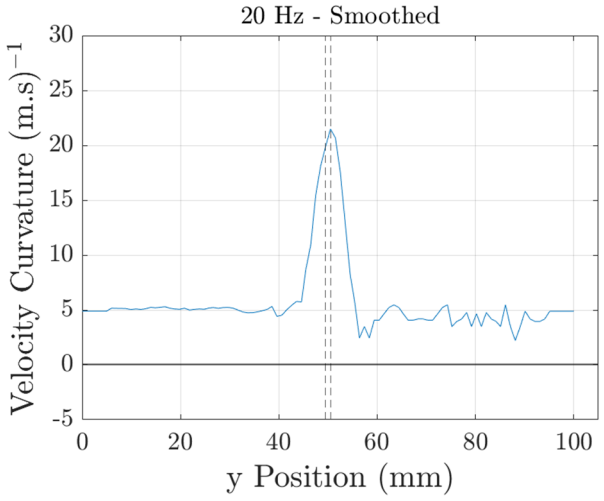

Figure 36: Velocity curvature for 1 mm notched beam at 20 Hz frequency from FEA simulation result

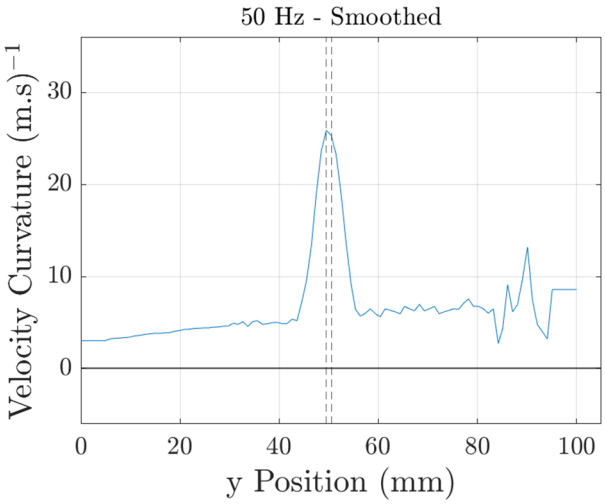

Figure 37: Velocity curvature for 1 mm notched beam at 50 Hz frequency from FEA simulation result

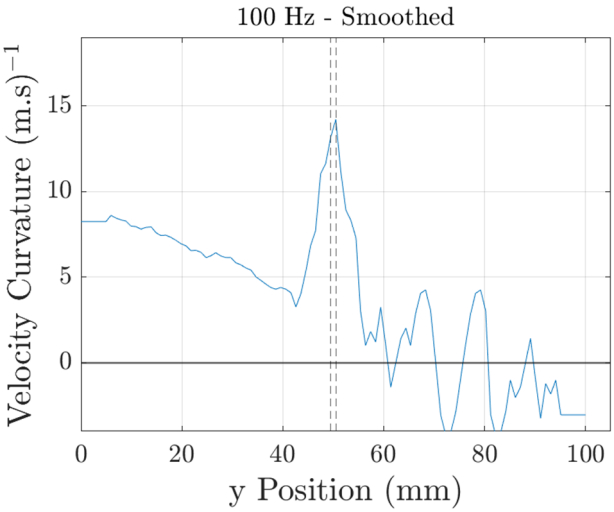

Figure 38: Velocity curvature for 1 mm notched beam at 100 Hz frequency from FEA simulation result

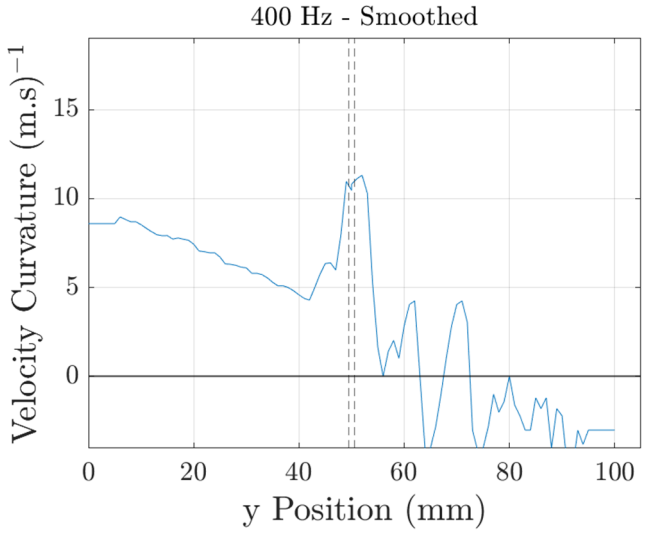

Figure 39: Velocity curvature for 1 mm notched beam at 400 Hz frequency from FEA simulation result

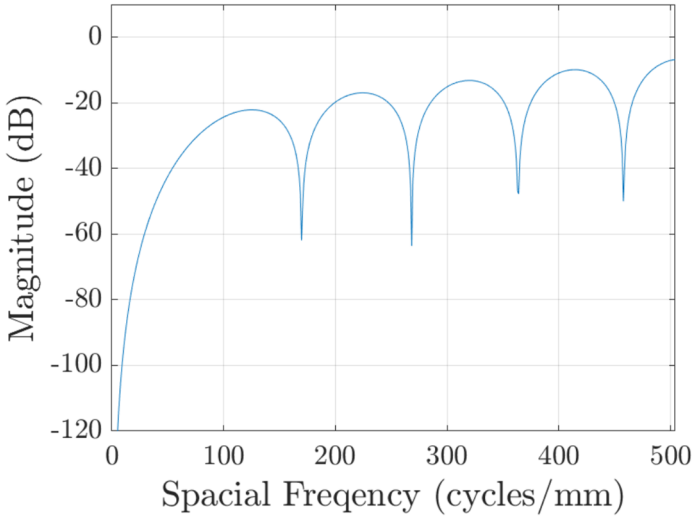

Figure 40: Magnitude reduction (dB) versus spatial frequency (cycles/mm)

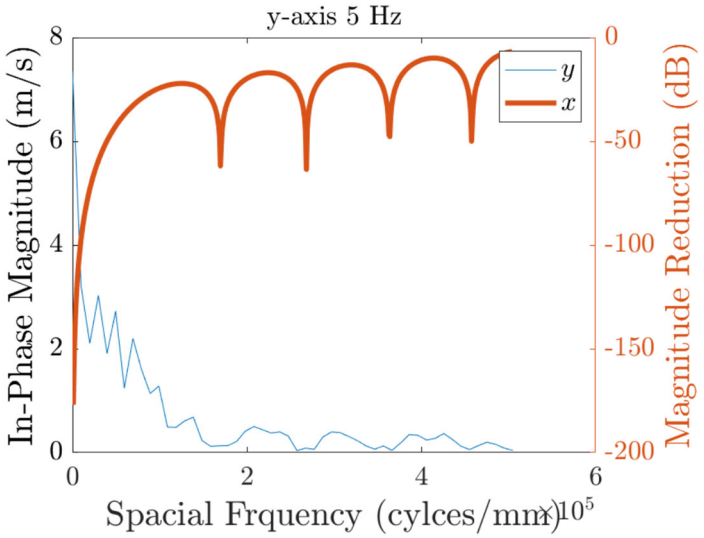

Figure 41: In-phase magnitude (m/s) and magnitude reduction (dB) vs. spatial frequency (cycles/mm) at 5 Hz

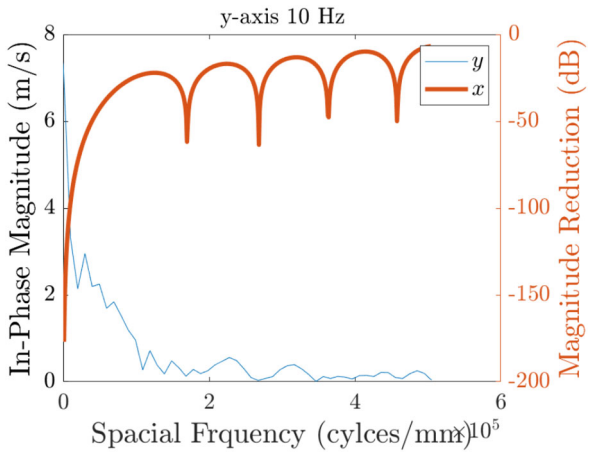

Figure 42: In-phase magnitude (m/s) and magnitude reduction (dB) vs. spatial frequency (cycles/mm) at 10 Hz

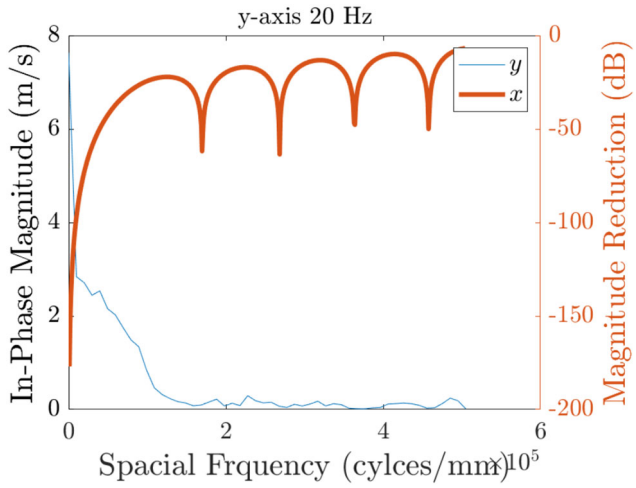

Figure 43: In-phase magnitude (m/s) and magnitude reduction (dB) vs. spatial frequency (cycles/mm) at 20 Hz

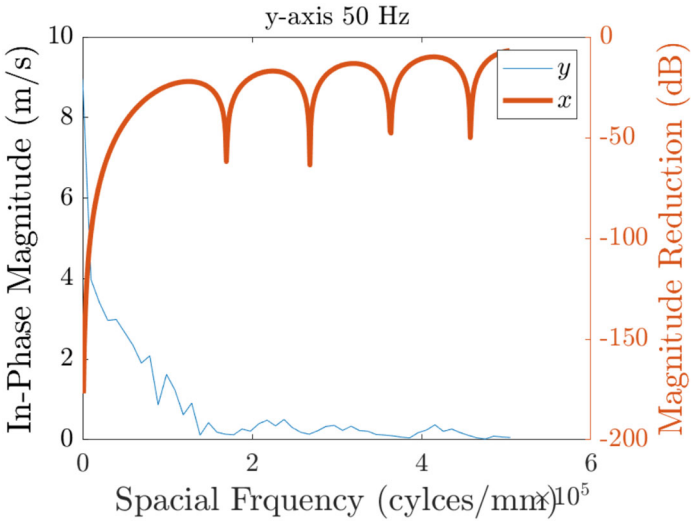

Figure 44: In-phase magnitude (m/s) and magnitude reduction (dB) vs. spatial frequency (cycles/mm) at 50 Hz

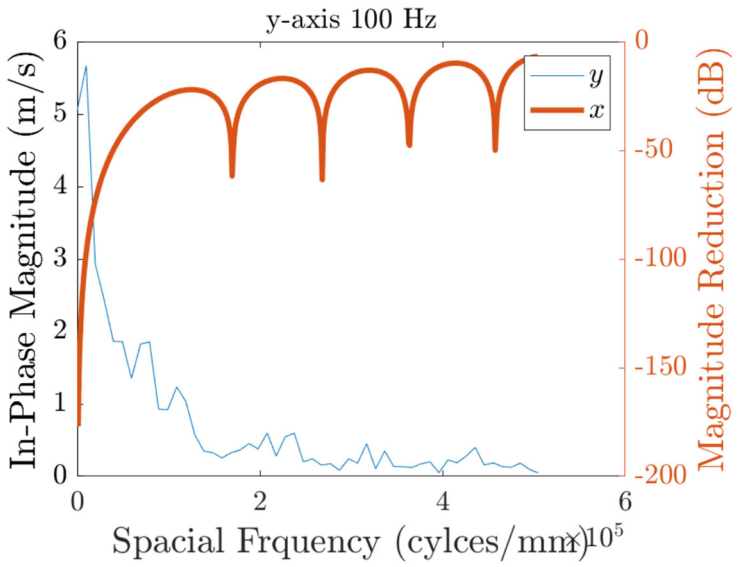

Figure 45: In-phase magnitude (m/s) and magnitude reduction (dB) vs. spatial frequency (cycles/mm) at 100 Hz

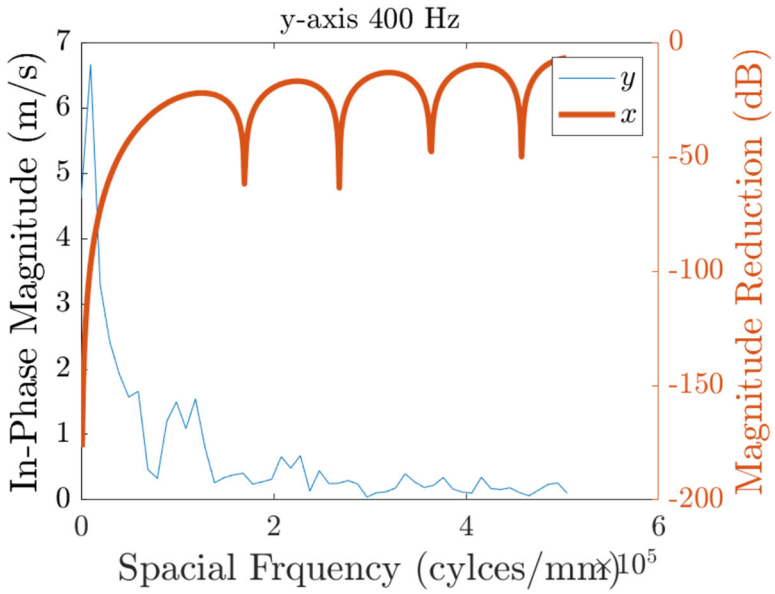

Figure 46: In-phase magnitude (m/s) and magnitude reduction (dB) vs. spatial frequency (cycles/mm) at 400 Hz